

Generating Laser Line of Diode Laser by Means of Powell Lens: Simulation and Experimental Results

Abolhasan Mobashery*, Seyed Ayoob Moosavi, and Mojtaba Arjmand

Faculty of Applied Science, Malek Ashtar University of Technology, Shahinshahr, Iran

Corresponding author email: ahmobi@mut.ac.ir

Received: July 9, 2024, Revised: May 01, 2025, Accepted: July 08, 2025, Available Online: July 10, 2025
DOI: will be added soon

ABSTRACT— In the present paper, the design of the laser transmitter section of a LiDAR system is described for autonomous vehicles. The optical system is designed to produce a linear laser beam with uniform intensity. The output beam from the diode laser has a non-uniform Gaussian profile. Conventional methods for converting this profile into a linear one often results in an uneven distribution along the line. In order to address this issue, a Powell lens is used. The Powell lens is an aspheric lens that transforms the incoming parallel beam into a linear beam with a uniform profile. In this type of lens, two parameters—the radius of curvature and the conic constant—must be selected to ensure uniform intensity across the entire laser line. In the present study, the diode laser intensity distribution, collimating lenses, and Powell lens are simulated using Zemax software. The collimating lens transforms the highly divergent laser beam into a nearly parallel beam, after which the Powell lens, with a radius of curvature of $r=0.9$ mm and a conic constant of -1.7 , produces a linear laser profile with a divergence angle of 60 degrees. Experimental results confirm the accuracy of the design and simulation process. In the experimental tests, the power drop of the laser at the start and end of the laser line was measured to be less than 15%.

Keywords: Powell lens, conic constant, uniform line beam, beam shaping, LiDAR

I. INTRODUCTION

High-power, nanosecond pulse lasers are key components of Light Detection and Ranging (LiDAR) systems. These elements are essential for autonomous driving and object detection [1]. In LiDAR systems for autonomous

vehicles, in order to prevent collisions with pedestrians and other objects, it is crucial to determine the distance and angle of surrounding objects in a continuous and accurate way. One of the common distance measurement methods is called the time-of-flight, which calculates distance by measuring the time taken for light emitted from a source to reflect off an object and return. In rangefinder systems, because of the low divergence of the laser beam and the narrow field of view in the receiver, a fast scanner or multiple rangefinders are required to cover the area around the vehicle.

For reducing the number of LiDAR systems and eliminating optomechanical systems responsible for beam scanning in front of the vehicle, it is preferable to convert the laser beam into a line. This linear beam can then be detected by an array of sensors to determine the distance and angular position of objects. However, due to the reduced beam intensity in this configuration, higher-power laser diodes are required.

Most lasers produce circular or elliptical beams with Gaussian or near-Gaussian intensity profiles. While a Gaussian intensity distribution is useful for applications that focus the laser beam to a small point, there are other applications where a uniform intensity distribution is more optimal. For instance, in material processing, a uniform intensity distribution ensures consistent exposure across the entire illuminated area [2-4]. Similarly, when laser light is used for illumination, a uniform beam profile is essential for consistent

illumination characteristics. This will simplify image processing by ensuring uniform brightness, regardless of the object's position in the illuminated area. Uniform illumination also enhances contrast and clarity [5-8].

Diffraction optics offers a highly effective tool for reshaping Gaussian intensity distributions. Specifically, these optics are used to produce nearly any desired intensity profile and a wide variety of patterns [9-11]. Diffraction optics work by creating interference between different diffraction orders to redistribute the incoming beam's intensity distribution. However, diffraction effects are inherently dependent on the wavelength. That is, a given diffractive element only operates within a narrow wavelength range. This wavelength sensitivity can be particularly problematic when pairing diffractive elements with diode lasers, as these lasers have a relatively broad wavelength bandwidth compared to other laser types. Additionally, there are considerable variations in nominal wavelength between lasers within a set. Diffractive optical elements (DOEs) inevitably direct some light into unwanted diffraction orders and generally have a limited working distance, outside of which the desired intensity pattern is not produced [12].

One of the common methods for generating a linear laser pattern is to use a cylindrical lens [13]. If we consider Gaussian laser emission and an ideal lens is used to expand the laser spot, the spot intensity will be high in the center and decrease towards the edges due to the non-uniform of laser beam distribution. Moreover, spherical aberration from the lens causes further expansion of the line edges. This will result in an additional intensity drop at the laser line's edges [13]. The edge intensity reduction in a LiDAR system's laser line reduces the power of the transmitted signal, thus decreasing the likelihood of detecting the received signal from those directions.

Another method for generating a laser line is to use a Powell lens. This method produces a laser line with a uniform intensity profile [5-8, 14-15]. The Powell lens resembles a prism, but with a small radius at the apex, this will cause

the spread of the laser beam only in one direction. In addition to creating a uniform linear pattern, this lens supports a lightweight and straightforward optical setup.

The present paper focuses on converting the asymmetric profile of a high-power four-channel diode laser into a symmetrical laser line. The simulations are conducted using ZEMAX software, and then validation is performed by experimental results. In Section 2, we explain the mathematical description of the Powell lens. Simulation of laser diode and optical elements will be discussed in Section 3. Section 4 contains the experimental results and the conclusion is presented in Section 5.

II. MATHEMATICAL DESCRIPTION OF POWELL'S LENS

In order to create a laser line pattern with uniform intensity, the central rays of the laser beam must experience greater divergence than the edge rays. In order to get this optical characteristic, we consider an optical element with a primary and a secondary surface. The primary surface of this optical element should be designed so that the rate of change in the slope of the rays is higher at the center of the surface, so that the faster divergence changes are seen in this central region. On the other hand, at the edges of this surface, the rate of slope change should be lower. The secondary surface of this optical element is designed to have no effect on beam uniformity; it induces simple refraction to increase the divergence of the rays without interfering with the uniformity of the beam distribution. One of the most important considerations in designing this element is the practical limitations of manufacturing. Any discontinuities on the surface should be avoided to ensure a smooth design.

The Powell lens is a cylindrical aspheric lens composed of a conical surface with a small radius of curvature and a relatively large conic constant, along with a flat surface. The conical surface in the (y, z) plane is described by the following equation [16]:

$$z = \frac{cr^2}{1 + (1 - (1 + Q)c^2 r^2)^{1/2}} \quad (1)$$

where $c = 1/R$ is the curvature of the surface, and Q is the conic constant. The design of such a lens depends on the laser beam diameter, the divergence of the output beam, the refractive index of the lens material, and the orientation of the lens relative to the incoming beam. For a given beam diameter, with the lens material identified and its refractive index known, only two parameters need to be considered: the radius of curvature and the conic constant. In the Powell lens, the value of Qc ranges between 0.25 and 50 [17,18].

In designing the Powell lens, if the beam diameter changes, the optimal radius also changes by the same factor, without any change to the conic constant. The numerical value of this product is unusual for ordinary optical surface. Optical systems typically consist of elements with spherical or flat surfaces. Aspheric surfaces generally have conic constants with magnitudes below 1. Only a small percentage of surfaces have conic constants with magnitudes greater than 1, and in such cases, their radius of curvature is typically greater than 10 mm. Thus, it is rare for an optical system to have surfaces with a conic constant and curvature product greater than, for example, 0.1. However, this characteristic is seen in the Powell lens.

A key point regarding the Powell lens is that the radius of curvature must be smaller than the input beam diameter. In this condition, the generated laser line is uniform. By decreasing the radius of curvature, the intensity distribution shifts toward the edges, while a larger radius shifts it toward the center of the line.

III. SIMULATIONS

A. Simulation of Laser Diode and Its Collimator

The diode laser considered for the LiDAR system is a 125 watt laser from OSRAM with a wavelength of 915 nm. This laser consists of four diode bars, providing the required power

for the LiDAR system. The specifications of this laser are shown in Table (1).

Table 1. Specifications of the considered Diode Laser.

Parameter	Value
Center wavelength	915 nm
Spectral bandwidth (FWHM)	8 nm
Number of channels	4
Peak output power	125 W
Beam divergence (FWHM) parallel to pn-junction	10 °
Beam divergence (FWHM) perpendicular to pn-junction	25 °
Laser aperture (FWHM) parallel to pn-junction	220 μm
Laser aperture (FWHM) perpendicular to pn-junction	10 μm

The beam pattern provided by the manufacturer enables simulation in Zemax software. The laser's output beam profile at a distance of 1.1 mm from the exit port of diode laser is shown in Fig. 1, where the beam profile of each laser bar can be observed.

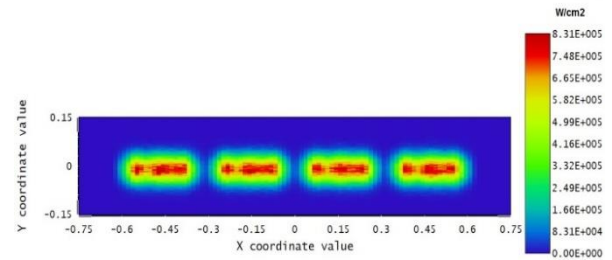


Fig. 1. Intensity pattern of laser bars at a distance of 1.1 mm from diode laser

The divergence of the laser output beam is approximately $25^\circ \times 10^\circ$. In order to put the Powell lens in front of the laser, the output beam must be collimated. For this purpose, an aspheric lens with the laser placed at its focal point is used. The collimating lens has a focal length of 4.05 mm, and its second surface being an even aspheric surface, described by the following equation [16]:

$$z = \frac{cr^2}{1 + (1 - (1 + Q)c^2 r^2)^{1/2}} + \alpha_1 r^2 + \alpha_2 r^4 + \alpha_3 r^6 + \alpha_4 r^8 + \alpha_5 r^{10} + \alpha_6 r^{12} + \alpha_7 r^{14} + \alpha_8 r^{16} \quad (2)$$

where the coefficient α_1 to α_8 are aspheric parameters that define departure from spherical

surface. In the simulation we used α_2 to α_5 in order to produce a collimated laser beam. The values of these parameters are given in Table 2. Using this lens, the beam divergence is reduced, resulting in beam dimensions of $3.8\text{mm} \times 2\text{mm}$ (H×V) after the collimating lens.

Table 2. the values of aspheric parameters of collimating lens.

Parameter	Value
α_1	0
α_2	-5.136×10^{-3}
α_3	-9.111×10^{-4}
α_4	1.138×10^{-4}
α_5	-4.15×10^{-5}
α_6	0
α_7	0
α_8	0

B. Powell lens simulation

In order to examine the effect of radius of curvature and conic constant of the Powell lens on the beam intensity uniformity, a Powell lens have been simulated in Zemax software. The specifications of the simulated Powell lens are presented in Table 3. The Powell lens simulation have been conducted in the non-sequential mode of Zemax using a Toroid surface, defined by Equation (1).

In this simulation, the conic constant has been initially set to -0.5, and the radius of curvature has been varied between 0.5 mm and 1.3 mm. The changes in the output beam profile from the Powell lens at a distance of 100 mm are shown in Fig. 2.

Analysis of the beam profile exiting the Powell lens shows that with a smaller radius of curvature, the beam intensity shifts toward the edges of the laser line and the beam divergence is larger than expected value. As the radius of Powell lens increases, the intensity distribution becomes gradually uniform and the beam divergence decreases, but with larger radius of curvature, the intensity distribution shifts toward the center of the laser line and the beam divergence angle of the beam becomes smaller.

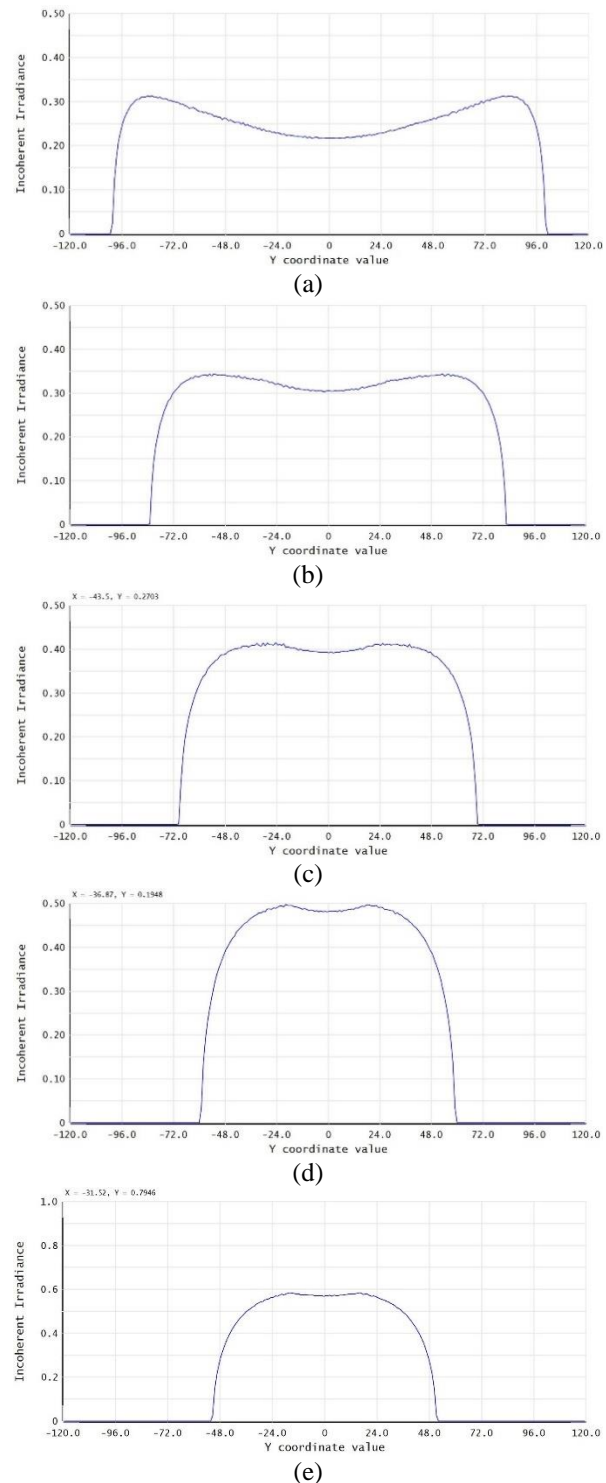


Fig. 2. The intensity distribution of the laser line after the Powell lens for (a) $r=0.5$ mm, (b) $r=0.7$ mm, (c) $r=0.9$ mm, (d) $r=1.1$ mm, (e) $r=1.3$ mm

In the second step, a radius of curvature of 0.9 mm has been chosen for the toroid surface, and the conic constant has been varied between -1.1 and -2.1. The results of these adjustments are shown in Fig. 3. As observed, increasing the absolute value of the conic constant shifts the spot intensity distribution from the center

towards the edges and the laser divergence decreases. Therefore, it is concluded that reducing the radius of curvature transfers energy towards the edges of laser line and increase the beam divergence, while increasing it focuses the beams towards the center and decrease the beam divergence. Also, lowering the absolute value of the conic constant concentrates the beam in the middle region of the line and decreases the beam divergence, while increasing this value causes a shift in the beams towards the edges of laser line and increase the beam divergence.

Table 3. Specifications of the Simulated Powell Lens.

Parameter	Value
Beam diameter	2 mm
Output beam divergence	60 o
Lens material	BK7
Wavelength	915 nm
Lens thickness	9 mm

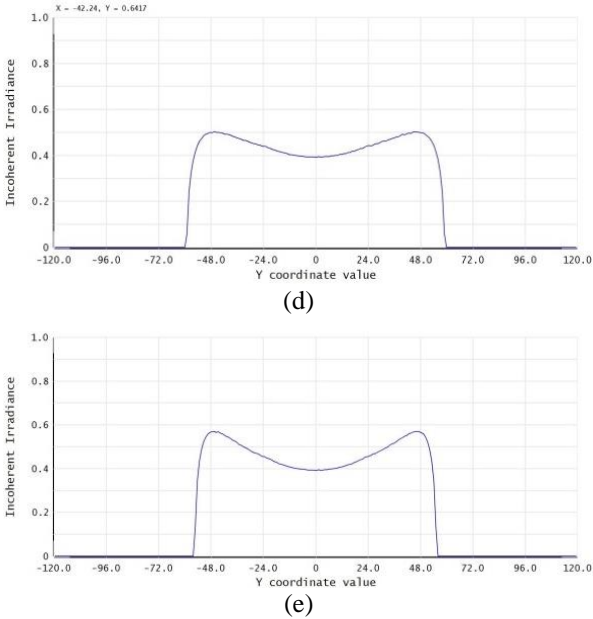
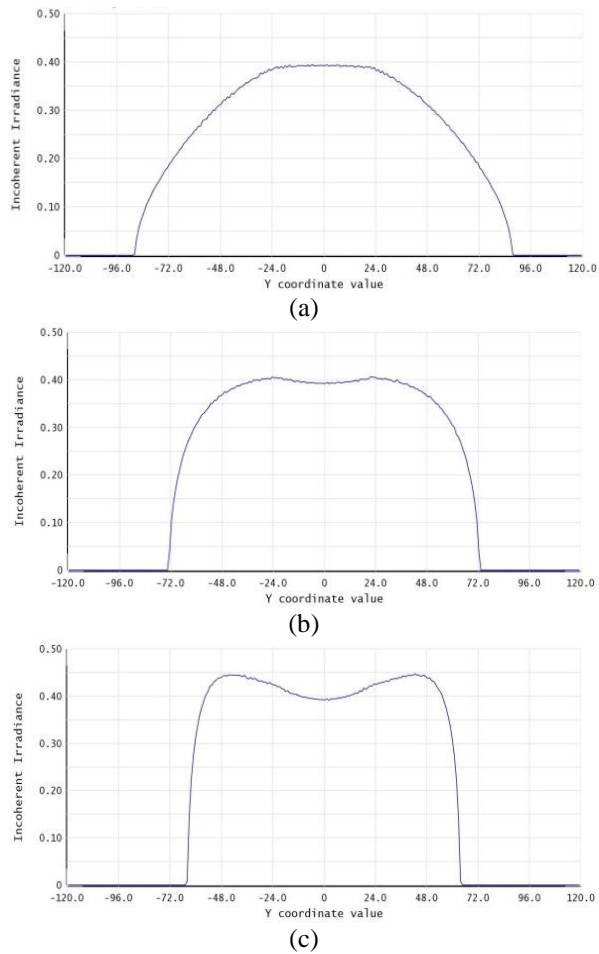


Fig. 3. The intensity distribution of the laser line after the Powell lens with $r=0.9$ mm and (a) $Q=-1.1$, (b) $Q=-1.4$, (c) $Q=-1.7$ mm , (d) $Q=-1.9$, and (e) $Q=-2.1$

Thus, in designing a Powell lens, the product of the conic constant and the surface radius of curvature is a critical factor in determining the intensity distribution of the laser line. In order to determine the final values for the radius of curvature and conic constant of the Powell lens, laser distribution has been considered as uniform along the line, so that only a 15% power difference between the edges and centre of the laser line has been allowed. Based on this criterion, the best intensity distribution has been achieved with a lens by radius of 0.9 mm and a conic constant of -1.7. Figure 4 shows the designed lens.

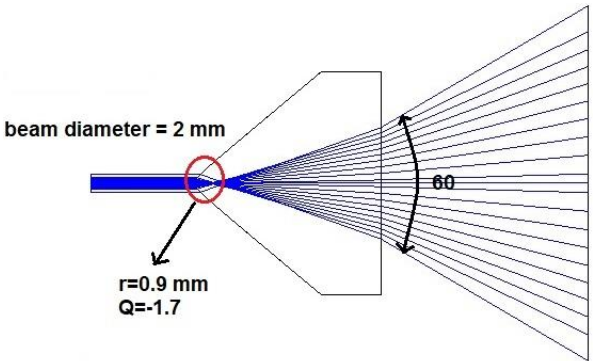


Fig. 4. Powell lens geometry for laser line generation.

After the collimating lens, the Powell lens is placed at the distance of 1.5 mm from the collimating lens. The Powell lens is aligned

such that its apex is oriented along the y-axis, which is the fast axis of the laser. Figure 5 illustrates the arrangement of the laser, collimating lens, and Powell lens. According to this setup, the Powell lens expands the laser beam along the x-axis, which is perpendicular to the plane.

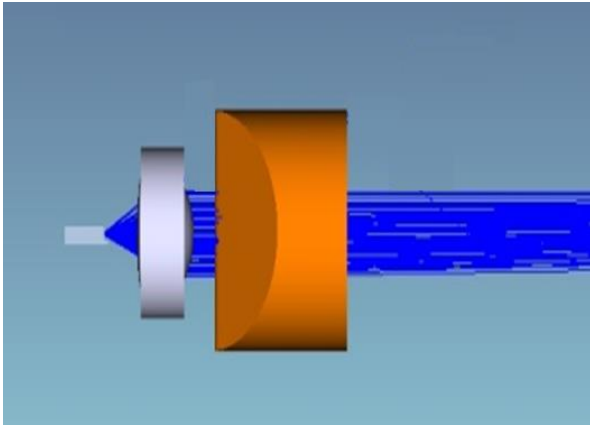


Fig. 5. Arrangement of laser diode, collimating lens and Powell lens in ZEMAX software

The laser beam intensity pattern at a distance of 150 mm from the laser is shown in Fig. 6. Based on this figure, the laser illuminates the target as a line with uniform intensity and a divergence angle of 60 degrees.

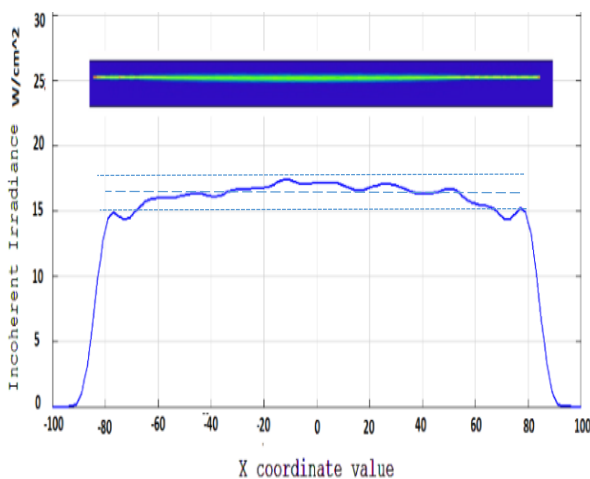


Fig. 6 Laser intensity pattern after Powell lens at a distance of 150 mm

IV. EXPERIMENTAL TESTS

Based on the simulations, the collimating and Powell lenses were purchased according to the software data and positioned in front of the diode laser. The results were then analyzed. Figure 7 shows the pattern obtained from the diode laser in the lab before the collimating

lens. In order to capture this intensity pattern, a microscope objective lens with a 40X magnification was used. This lens projected the cross-section of the diode laser output onto a screen placed at the distance of 160 mm. A CCD camera without an IR cut filter captured the image of the laser spot on the screen. Since the CCD camera's front lenses were non-removable, it could not be used directly in the optical setup, and the laser pattern on the screen was recorded and displayed by the camera.

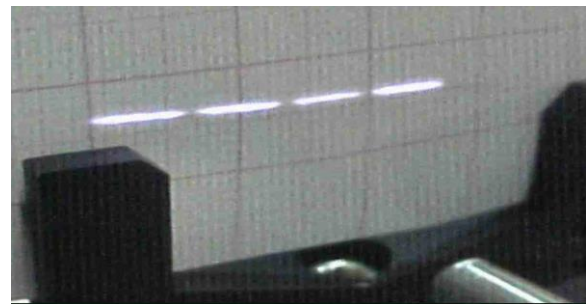


Fig. 7 Magnified near field pattern of the laser beam

After placing the collimating lens, a small laser spot was formed at a distance of 50 mm, as shown in Fig. 8. As observed, the laser spot appears as an ellipse along the laser's slow axis. The beam diameter upon exiting the collimating lens is 2 mm, matching the input beam diameter to the Powell lens in the previous simulation section. Hence, with the Powell lens positioned after the collimating lens, the desired linear beam profile was achieved. Figure 9 shows the laser profile at a distance of 150 mm from the laser.



Fig. 8. Laser beam profile at a distance of 50 mm from the collimating lens

Laser power measurements at various points along the laser line reveal that the intensity drop at the line edges is less than 15%. The intensity was measured using a photodiode, which was moved along the laser line, recording intensity

at 10 mm intervals. This intensity profile is displayed in Fig. 9.

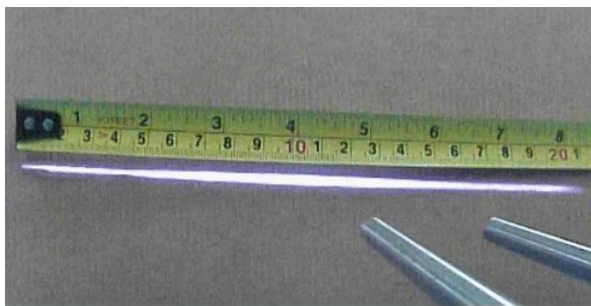


Fig. 9 Uniform laser line produced at a distance of 150 mm from the diode laser

V. CONCLUSION

The Powell lens is a cylindrical aspheric lens that converts an incoming laser beam into a uniform linear distribution. The radius of curvature of the aspheric region of Powell lens is very small, and its conic constant is relatively large. Simulations showed that if the aspheric region of lens (radius of curvature of lens) is too small, the highest intensity shifts towards the edges of the output beam, and resulting in a completely non-uniform intensity distribution. As the radius of curvature increases, the intensity distribution becomes more uniform. Optimal uniformity is achieved when the width of the curved region of the lens is slightly smaller than the laser spot dimensions. If the width of this region exceeds the diameter of the incoming beam, the edges of the beam become narrower, and the central intensity of laser line increases.

In the present investigation, a diode laser profile was transformed into a laser line using a Powell lens. In this process, a collimating lens with $f = 4.5$ mm converted the nonuniform beam of laser bar into a spot of 2mm x 3.8 mm. The Powell lens, with a radius of curvature of 0.9 mm and a conic constant of -1.7 converted the laser beam into a laser line with a 60-degree divergence angle. Throughout this process, the laser power drop at the line edges was measured to be less than 15%.

REFERENCES

Y Li and J Ibanez-Guzman, "LiDAR for autonomous driving: The principles, challenges, and trends for automotive lidar and perception

systems," *IEEE Signal Process. Mag.*, Vol. 37, pp. 50-61, 2020.

H. Liu, X. Qin, S. Huang, Z. Hu, and M. Ni, "Geometry modeling of single track cladding deposited by high power diode laser with rectangular beam spot," *Opt. Lasers Eng.*, Vol. 100, pp. 38-46, 2018.

S.L. Campanelli, A. Angelastro, P. Posa, and G. Daurelio, "Fiber laser surface remelting of a nickel-based superalloy by an integrated rectangular laser spot," *Opt. Lasers Eng.*, Vol. 111, pp. 42-49, 2018,

S. Akhtar, O. Ozgur Kardas, O. Keles, and B. Sami Yilbas, "Laser cutting of rectangular geometry into aluminum alloy: Effect of cut sizes on thermal stress field," *Opt. Lasers Eng.*, Vol. 61, pp. 57-66, 2014,

K. Chen, W. Song, L. Han, and K. Bizheva, "Powell lens-based line-field spectral domain optical coherence tomography system for cellular resolution imaging of biological tissue," *Biomed Opt Express*. Vol. 14, pp. 2003-2014, 2023.

K. Chen, N. Abbasi, A. Wong, and K. Bizheva, "In vivo, contactless, cellular resolution imaging of the human cornea with Powell lens based line field OCT," *Sci Rep*. Vol. 14, pp. 22553(1-11), 2024.

S. Saghafi, K. Becker, C. Hahn, and H.U. Dodt, "3D-ultramicroscopy utilizing aspheric optics," *J Biophoton.*, Vol. 7, pp. 117-125, 2013.

S. Saghafi, K. Becker, N. Jährling, M. Richter, E.R. Kramer, and H.U. Dodt, "Image enhancement in ultramicroscopy by improved laser light sheets," *J Biophoton.*, Vol. 3, pp. 688-695, 2010.

L.L. Doskolovich, A.A. Mingazov, E.V. Byzov, R.V. Skidanov, S.V. Ganchevskaya, D.A. Bykov, E.A. Bezus, V.V. Podlipnov, A.P. Porfirev, and N.L. Kazanskiy, "Hybrid design of diffractive optical elements for optical beam shaping," *Opt. Express*, Vol. 29, pp. 31875-31890, 2021.

S. Katz, N. Kaplan, and I. Grossinger, "Using Diffractive Optical Elements: DOEs for beam shaping—fundamentals and applications," *Opt. Photonik*, Vol. 13(4), pp. 83–86, 2018.

A. Siemion, "Terahertz diffractive optics—smart control over radiation," *J. Infrared, Millimeter, Terahertz Waves*, Vol. 40(5), pp. 477–499, 2019.

Y. Chen, F. Wang, and Y. Cai, "Partially coherent light beam shaping via complex spatial coherence structure engineering," *Adv. Phys.* Vol. 7, pp. 1-30, 2021.

H. Sun, *A Practical Guide to Handling Laser Diode Beams*, New York: Springer Dordrecht Heidelberg, Ch. 3, 2015.

S. Foroughipour, K. Becker, M. Foroughipour, N. Ghaffari Tabrizi-Wizsy, N. Sarem, C. Fuchssteiner, and S. Saghafi, "Converting a symmetrical Gaussian beam into a thin tunable light shee," *Methods Microscopy*, Vol. 1, pp. 65-75, 2024.

R. Chen, X. Li, X. Wang, J. Li, G. Xue, Q. Zhou, and K. Ni, "A planar-pattern-based calibration method for high-precision structured laser triangulation measurement," *Proc. SPIE, Optical Metrology and Inspection for Industrial Applications* Vol. 1118914, 2019.

Ansys ZEMAX opticstudio, *Optical Design Program User's Manual*, 2023.

I. Powel, "liner diverging lens," US patent, 4828299, 1989.

S.M. Ranjbaran, K. Kratkiewicz, R. Manwar, and K. Avanaki, "Line Illumination in Linear Array Photoacoustic Imaging Using a Powell Lens: A Proof-of-Concept Study," *Photonics*, Vol. 11(4), pp. 288(1-13), 2024.

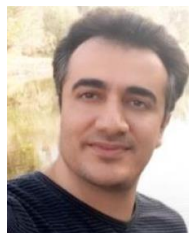


Abolhasan Mobashery completed his B.Sc. at Shiraz University, Shiraz, Iran, an M.Sc. and Ph.D. at Isfahan University, Isfahan, Iran in atomic and molecular physics. His main research works are in laser spectroscopy and Adaptive Optics. His research interests are in beam shaping, optical communication and optical vortex. He is an Assistant Professor at Malek Ashtar University of Technology. Dr. Mobashery is a member of Physics Society of Iran and Optics and Photonics Society of Iran.



Mojtaba Arjmand received the B.Sc. degree in applied physics in 2008, and the M.Sc. degree in optoelectronics engineering in 2011. In 2016, he received a PhD in applied physics from University of Isfahan, Isfahan, Iran.

He spent a six months visiting scholar at Istituto di Fisica Applicata "Nello Carrara" (IFAC-CNR), Sesto Fiorentino, Italy in 2015. His research activity was done at Chemical and Biochemical Optical Sensor Group where they develop the optical long-period fiber grating and surface plasmon resonance based fiber sensors for bio applications. Currently, he is an assistant professor at Malek Ashtar University of Technology. His research interests include SPR and fiber optic label-free biosensor, FBG and fiber grating based sensors, microfiber technology, and LiDAR based remote sensing. Dr. Arjmand is a member of Optics and Photonics Society of Iran (OPSI) and Physics Society of Iran (PSI).



Seyed Ayoob Moosavi received his B.Sc. degree in applied physics from Yazd University, Yazd, Iran in 2007, the M.Sc. degree in photonics from Graduate University of Advanced Technology, Kerman, Iran in 2010, and his Ph.D. degree in physics in the field of laser from Malek Ashtar University of Technology, Isfahan, Iran in 2019. His research interests are in the areas of Adaptive Optics, OAM communication, and free space optical communication.